CCUS: 4186259

Active Source Sparse Imaging Using Permanent SADAR Arrays

Derek Quigley*[1], Paul A. Nyffenegger[2], Kevin D. Hutchenson[2], Jonathan Yelton[1]
1. Quantum Technology Sciences, 2. Geospace Technologies and Quantum Technology Sciences.

This paper was prepared for presentation at the Carbon Capture, Utilization, and Storage conference held in Houston, TX, 03-05 March.

Abstract

Quantum Technology Sciences installed a network of four dual-use permanent compact volumetric phased arrays (SADAR arrays) at Carbon Management Canada's Field Research Station to demonstrate capabilities for seismic monitoring and verification at an active geologic CO_2 storage facility. The SADAR network is designed to meet microseismic monitoring requirements, but we also demonstrate the arrays effectiveness for verifying reservoir conformance using active source sparse imaging. We demonstrate the imaging capability robustness and stability against loss of multiple sensors.

Introduction

In November 2021 Quantum Technology Sciences Inc. (QTSI) installed a sparse network of four permanent compact volumetric phased arrays (SADAR arrays) at Carbon Management Canada's Newell County Field Research Station (FRS) proving ground for geologic carbon storage (GCS) technologies to demonstrate the use of the SADAR arrays for monitoring, measurement, and verification (MMV) (Nyffenegger *et al*., 2022). The FRS, located in Southern Alberta (Figure 1), provides an active GCS test site regularly injecting a controlled volume of CO_2 into the Basal Belly River Sandstone (BBRS, z=300 m) enabling testing and evaluation of MMV (Lawton *et al*., 2019; Macquet *et al.*, 2022).

SADAR arrays are designed to provide a complete volumetric sampling of the propagating wavefield across the array, enabling coherent array processing techniques, suppressing noise, and allowing separation of signals with different propagation parameters (Nyffenegger *et al*., 2023; Zhang *et al*., 2023). The SADAR arrays installed at the FRS consist of 50-72 GS-ONE vertical geophones grouted into shallow boreholes at between 9m-19m depths below the weathering layer; the position of each array element is known to an accuracy of several centimeters. The boreholes for each SADAR array are uniformly spaced into arrangements of cylindrical shells. The installation of the four arrays, a total of 231 elements comprised of vertical geophones, and all supporting equipment from start to finish lasted about a week. Since then, the SADAR network has been acquiring data at 2000 samples per second at a 98.7% reliability rate and performing ongoing microseismic monitoring at the site (Hutchenson *et al.*, 2024; Nyffenegger *et al.*, 2025).

Although the SADAR systems and network are designed to meet microseismic monitoring requirements, the network simultaneously records Vibroseis monitoring surveys, providing a dual-use as an effective tool for verifying reservoir conformance in an active source, sparse imaging context. We present results that showcase SADAR capabilities for imaging. We demonstrate benefits of higher density receiver gathers using conventional processing methods, and improvement using beamforming to target specular reflections from specific survey geometries. We also demonstrate that images built from beamformed data are robust to sensor attrition. The SADAR arrays and beamformed images therefore ensure operational integrity over long duration deployments while also enabling time-lapse analysis with reduced effort.

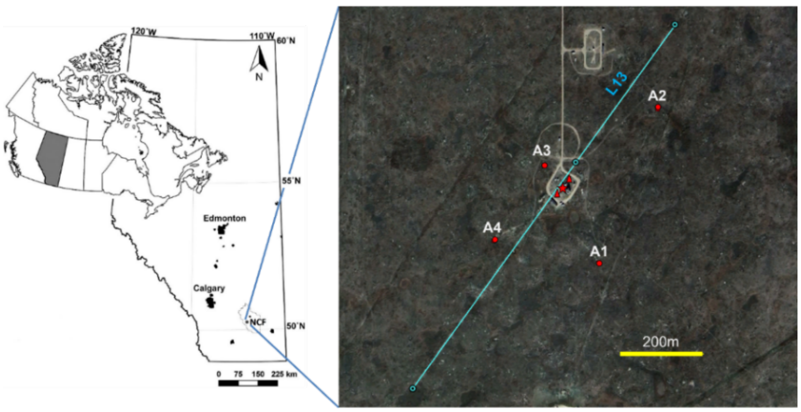

Figure 1. Map of Carbon Management Canada's Newell County Field Research Station in Alberta, Canada [Macquet et al., 2022]. The red star at center shows the CO_2 injection well location relative to the four SADAR monitoring arrays (red dots, A1-A4) and two monitor wells (red triangles). Location of the L13 Vibroseis survey line is shown in blue.

Methods

Since installation of the SADAR network at the NCF field site in November 2021, several seismic monitoring Vibroseis survey lines have been acquired. Data segments extracted from the continuously recorded passive network at the survey shot times can be used in a conventional reflection seismic processing sequence of 1) cross correlation of the recorded data segments, 2) averaging repeated shots from the same stations, 3) sorting into common receiver gathers of averaged shots to form a representative subsurface cross section, and 4) follow on image enhancement techniques.

Figure 2 (left) illustrates phase arrivals separating in time in a single sensor receiver gather. As is typical, slower air waves and ground roll arriving after initial reflections and refractions creates a noise cone that leaves an optimum offset window of clean data outside the cone (Hunter and Pullan, 1989). This optimum offset range provides a sparse yet clean image of a limited extent of the geologic horizons.

Single sensor common receiver gathers can be combined into a "super gather" for each array achieving a higher spatial sampling (Figure 2, center). Super gathers are created by stacking the vertical column of the arrays into one or more receiver groups and then binning midpoints similar to conventional procedures. Such a super gathered shot line is a narrow 3D swath rather than a standard 2D receiver gather cross section. The swath is irregularly sampled *i.e.* not on a rectangular grid, so standard practice includes interpolation to a regular geometry. For the case shown in Figure 2 (center) the super gather of A3 results in 17 traces per shot point.

Coherent processing of the phased array data to form beams provides a different processing path to higher quality optimum offset images. We demonstrate the improvement for receiver gather images using beamforming to target signals from specific reflection points per shot point. For the case of seismic reflections from active source surveys, the ideal beam's main response axis (MRA) points along the angle of arrival of the specular reflections originating from the reflection point at depth.

For each shot point and for each array, we form targeted beams for a z=500m reflector (~0.85 s two-way travel-time, previously identified with the Lower Mannville group) by applying time shifts to the individual array sensors prior to averaging. The time shifts are model based, computed by ray tracing from each targeted reflection point through a layered 1D depth velocity model to determine the angle and arrival time at each array element, and then calculate the time difference of arrival between the individual element and a reference position located at the centroid of each array. Targeted beamforming results in a single high SNR trace per shot point (Figure 2, right) through suppressing both random and coherent noise corresponding with other arrival angles and phase velocities.

Lastly, because sensor loss and impact on capabilities is a concern for long term monitoring, attrition of multiple array elements is investigated. The tolerance of the array to loss of multiple sensors is demonstrated by randomly removing individual array elements cumulatively and then generating the super-gather and targeted beam images for comparison with the baseline images.

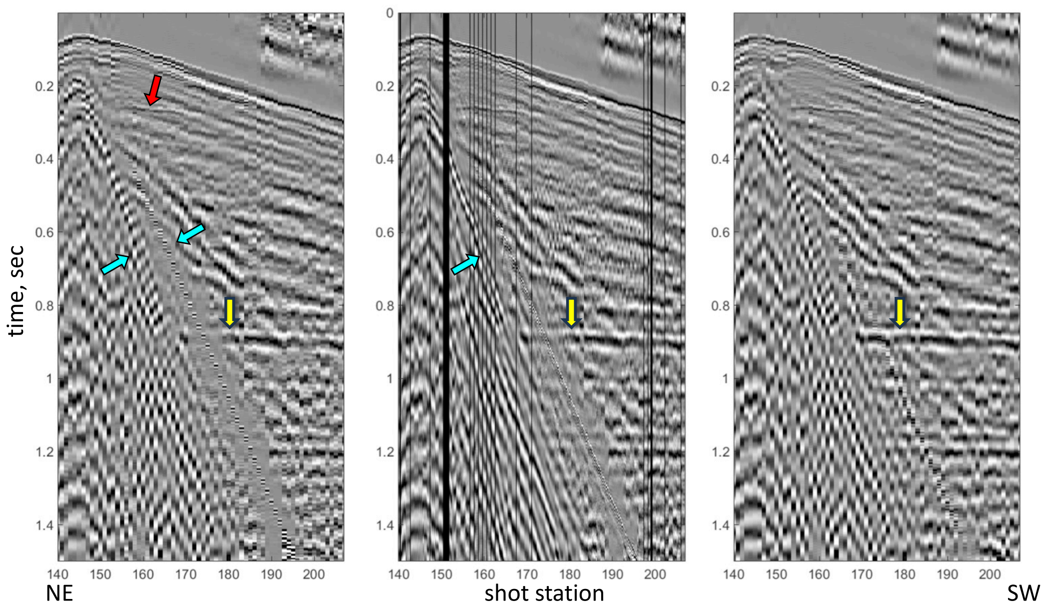

Figure 2. Common receiver gather images for Vibroseis line L13 from July 2022, for SADAR array A3. Displayed is: (left) single reference sensor gather, (center) super gather swath built from individual elements, and (right) corresponding beamformed gather image. For the super gather, gaps are shown where inline trace spacing exceeds 1m. Note the improvement in the coherence of flatter events at 0.25 s, 0.85 s, and 1.2 s and the attenuation of the air wave arrival relative to the single reference sensor image. Red arrow indicates the shallow BBRS reservoir, yellow arrows indicate the deeper ~0.85 sec reflector, and cyan arrows indicate the extent of ground roll and air wave signals.

Results

Figure 2 shows a comparison of data extracted from the SADAR passive monitoring network during the Vibroseis monitoring survey from July 2022 for SADAR array A3 for a subset of shot line L13. On the left is the common receiver gather for a reference sensor located at the center of A3. The center plot shows the corresponding super gather image, resulting in a finer, though irregular, lateral spatial sampling. The super gather image in Figure 2 shows the center "inline" bins of the super gather swath within 1m tolerance. This super gather demonstrates the ability to address aliasing of steeply dipping surface wave arrivals by reorganizing the data to improve the lateral spatial sampling.

The Figure 2 (right) plot illustrates the targeted beam image focusing on reflection points for the 0.85 s horizon. The noise suppression and spatial filtering provided by beamforming improves the sharpness of the targeted beam image. Because the beams in this image are based on angles of arrival for specular reflections, the same beam formulation serves to improve the BBRS reservoir image at ~0.25 s. In addition, suppression of the air-wave/ground-roll allows improving the SNR at stations 170-180 such that the targeted horizon is imaged where prior to beamforming no useful image was present. The beamformed receiver gather thus improves the capability for imaging the reservoir into the noise-dominated cone, expanding the available optimum offset window.

Sample images for SADAR array A3 considering the loss of 30 randomly selected sensors out of 51 total are shown in Figure 3. The super gather (Figure 3, left) shows an increasing number of gaps for missing traces as expected; observed aliasing for steeply dipping surface wave arrivals reappears. However, the targeted beam receiver gather shows little degradation compared with the equivalent image in Figure 2. Expected SNR loss in the targeted beams is less than 4 dB .

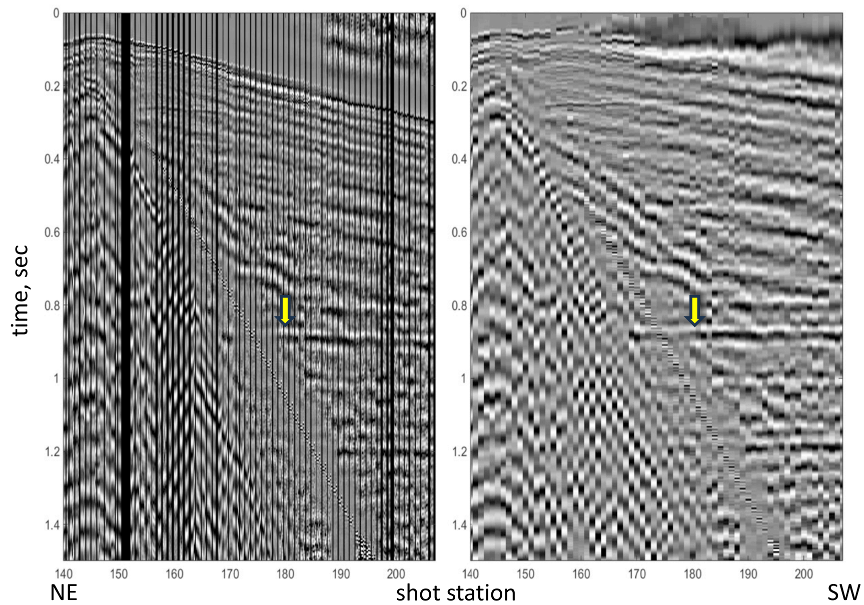

Figure 3. Receiver gather images for Vibroseis line L13 from July 2022 with 30 sensors randomly removed. (Left) Super gather swath from individual sensors and (right) targeted beamformed image. Yellow arrow annotations are the same as previous figure.

Discussion and Conclusions

Compared to standard surface sensors, data acquired using the permanent SADAR passive microseismic monitoring network during an active-source survey demonstrates significant signal improvement. These initial improvements are attributable to the array emplacement in boreholes below the weathering layer. Additionally, as Figure 2 demonstrates, the resolution and continuity of the structures in the targeted beam optimum-offset image focusing on specular reflections are superior to more conventional images created from individual channels. This enhancement is attributed to the noise suppression and spatial filtering beamforming provides.

Ensuring monitoring system capabilities is essential for guaranteeing operational integrity of GCS facilities over the required extended time spans. Impact of loss of sensors on imaging capabilities depends on phased array design, but Figure 3 demonstrates targeted beam imaging using data provided by SADAR arrays is tolerant to loss of individual sensors, even in the extreme case of over 50% attrition. The enhanced SNR and stability of the targeted beam image even to sensor loss will provide time and effort savings for timelapse analysis processing. Continuing investigation is needed to establish thresholds required for change detection using these methods.

This demonstration of imaging using SADAR arrays proves the systems' dual-use capability for both passive and active-source seismic GCS monitoring. The arrays are shown to be robust in tolerating sensor loss which reduces the technical and operational risks in long term monitoring. Altogether, because of the dual-use capability, the reduced footprint, and the robust design and system components, seismic MMV using SADAR systems decreases overall operator risks by supplying a single permanently emplaced system that guarantees reliability for long-term geologic asset management.

Acknowledgements

Quantum Technology Sciences, Inc., is a wholly owned subsidiary of Geospace Technologies Corporation, Inc. We acknowledge CMC for providing access to the CaMI Newell County Facility to enable installation of the SADAR system, and for sharing the data from the surface and downhole networks. The Newell County Facility is supported by funding from the Global Research Initiative at the University of Calgary from the Canada First Research Excellence Fund and from the CaMI Joint Industry Project. CMC is also acknowledged for providing operational data from the site.

References

Hunter, J. A., and Pullan, S. E., 1989, The optimum offset shallow seismic reflection technique: Proceedings of the Symposium on the Application of Geophysics to Engineering and Environmental Problems, EEGS, 143-174.

Hutchenson, K.D., D. Quigley, J. Longbow, E.B. Grant, P.A. Nyffenegger, J. Jennings, M.A. Tinker, M. Dahl, D. Grindell, M. Macquet, and D.C. Lawton, 2023, Microseismic monitoring using SADAR arrays at the Newell County carbon storage facility: what have we learned in a year?: Presented at GeoConvention, 2023, Calgary.

Lawton, D.C., J. Dongas, K. Osadetz, A. Saeedfar, and M. Macquet, 2019, Chapter 16: Development and analysis of a geostatic model for shallow CO2 injection at the Field Research Station, Southern Alberta, Canada, *in* T. Davis, M. Landro, and M. Wilson, eds., Geophysics and Geosequestration: Cambridge University Press, 280-296. DOI 10.1017/9781316480724.017.

Macquet, M., Lawton, L., Osadetz, K., Maidment, G., Bertram, M., Hall, K., Kolkman-Quinn, B., Parra, J. M., Race, F., Savard, G., and Wang, Y., 2022, Overview of Carbon Management Canada's pilot-scale CO_2 injection site for developing and testing monitoring technologies for carbon capture and storage, and methane detection: CSEG RECORDER, **47**(1), 1-27.

Nyffenegger, P.A., D.C. Lawton, M. Macquet, D. Quigley, B. Kolkman-Quinn, and K.D. Hutchenson, 2025, Advances in coupled passive and active seismic monitoring for large-scale geologic carbon storage projects, *in* Wilson, M., T. Davis, and M. Landro, eds., Geophysics and the Energy Transition: Elsevier Press, 333-354.

Nyffenegger, P.A., J. Zhang, E.B. Grant, D. Quigley, K.D. Hutchenson, M.A. Tinker, D.C. Lawton, and M. Macquet, 2023, Performance and outlook for the SADAR array network at the Newell County Facility: First Break, **41**, 56-62.

Nyffenegger, P.A., M.A. Tinker, J. Zhang, E.B. Grant, K.D. Hutchenson, and D.C. Lawton, 2022, Compact phased arrays for microseismic monitoring: First Break, **40**, 69-74.

Zhang, J., Hutchenson, K.D., Nyffenegger, P.A., Grant, E.B., Jennings, J., Tinker, M., Macquet, M. and Lawton, D.C., 2023. Performance comparison of compact phased arrays and traditional seismic networks for microseismic monitoring at a CO_2 sequestration test site: The Leading Edge, **42**(5), 332-342.